Int. J. Dynam. Control (2017) 5:903–916
DOI 10.1007/s40435-016-0234-1

Global dynamics of a prey-predator model with Allee effect and additional food for the predators

Kiran Kumar Gurubilli[1] · **P. D. N. Srinivasu**[2] · **Malay Banerjee**[1]

Received: 15 December 2015 / Revised: 12 February 2016 / Accepted: 16 February 2016 / Published online: 27 February 2016

Abstract Provision of additional/alternative food to the predators for controlling predator-prey dynamics has been receiving considerable attention from theoretical as well as experimental biologists. This is due to environment friendly role played by the additional food in controlling and managing the interacting population. Theoretical investigations done on additional food provided predator-prey models reveal that provision of additional food to predators has a significant role to play in enhancement of commercially important predator species and also in reduction of prey population. The quality and quantity of the additional food provided to predators play vital role in shaping the dynamics of the interacting system. So far as our knowledge goes, all theoretical investigations carried out in this direction assume logistic growth for the prey species. In reality, the per capita growth rate of the prey population is often an increasing function at low prey density. Incorporation of this realistic growth rate induces Allee effect into the dynamics of the prey species. In this paper, we consider an additional food provided predator-prey model wherein the prey population is subjected to Allee effect. The model includes both strong and weak Allee effects. This article presents a comprehensive analysis of the considered model that highlights the influence of Allee effect in prey and additional food for the predators on the system dynamics.

Keywords Stability · Local bifurcation · Global bifurcation · Heteroclinic orbit

✉ Malay Banerjee
malayb@iitk.ac.in

[1] Department of Mathematics and Statistics, I.I.T. Kanpur, Kanpur 208016, India

[2] Department of Mathematics, Andhra University, Visakhapatnam 530003, India

1 Introduction

Representing dynamics of population through mathematical models seem to have been initiated by Malthus in early nineteenth century through the development of Malthusian's model. This model was subsequently modified by introducing linear per-capita growth rate for the population which resulted in the well known logistic model. This modification allowed the population to evolve in such a way that it tends asymptotically to a constant termed as *carrying capacity* of the environment for the population [1]. In the early twentieth century, Lotka and Volterra independently developed models representing predator—prey interactions. Subsequently, this Lotka–Volterra model has been subjected to several modifications to incorporate the complex relationships that exist between the interacting species. For example, a variety of species dependent functional responses have been developed that enabled realistic representation of the interactions between prey and predator species [2–5]. Similarly, growth rate of the prey species has also been subjected to modifications through incorporation of various Allee effects such as additive Allee effect [6] and multiplicative Allee effect [7]. Although these attempts bring in complexities into the system dynamics, they draw the models closer to reality.

Allee effect is a realistic phenomenon that finds its presence in many fields associated with evolutionary biology. This concept has been formalised and initiated by the work of W.C. Allee in the early twentieth century [8]. Essentially, Allee effect refers to reduction in individual fitness at low population size or density [9]. This effect plays very important role in population dynamics. There are several mechanisms which generate Allee effect in population growth. A classification of various Allee effects characterised by the nature of involved mechanisms is presented in [10].

There are some real world examples [9,11–16] where the presence of Allee effect is observed. Consequently, analysis of systems involving Allee effect has gained lot of importance in problems associated with various fields such as conservation biology [17,18], sustainable harvesting [19], pest control, biological control [20], population management [10], biological invasions [21–25], metapopulation dynamics [26,27], interacting species [28–32]. The review article [33] presents a classification of single species models that are subjected to various Allee effects. Elaborate discussion on Allee effect can be found in the recent article [8]. Although there are many classifications within Allee effect such as strong Allee effect, weak Allee effect, demographic Allee effect etc., dynamics of population in presence of strong and weak Allee effects have been subjected to lot of investigations both mathematically [7,34–40] and ecologically [8,41].

Another important concept which is being investigated in the recent past is the dynamics of predator-prey systems when the predator is provided with additional food [42–45]. This concept deserves attention as many predators are more often found to be generalists rather than specialists. Moreover, provision of additional food to one of the interacting species has become an eco-friendly practice in the fields such as biological conservation, bio-remediation, resource management, biological control, pest management etc. Thus studying predator-prey dynamics when the predator is provided with additional food, following consequent changes in qualitative behaviour of the system and its dependance on the characteristics of the additional food such as quality and quantity would not only be mathematically interesting but also of practical importance.

In this article, we consider a predator-prey system where the growth of the prey species is influenced by Allee effect and the predator population is provided with additional food. The considered model can be made to exhibit both strong as well as weak Allee effect with appropriate choice on Allee effect parameter value. Our interest is to understand the role of additional food on the predator-prey dynamics. Comparing the considered system dynamics with the one without additional food reveals several interesting consequences which can be utilised for the purpose of biological control and species conservation.

This article is organised as follows. Section 2 introduces the model and presents a simplified version through the process of non-dimensionalisation. Section 3 presents equilibrium analysis and occurrence of local bifurcations. Global dynamics of the system are demonstrated through bifurcation diagrams and phase portraits in Sect. 4. This is followed by discussion section. The analysis pertaining to various local bifurcations is presented in the "Appendix".

2 Model

In this paper we consider the following nonlinear system which represents predator-prey interactions

$$\frac{dN}{dT} = rN(N-L)\left(1-\frac{N}{K}\right) - g(N,P,A)P, \tag{1}$$

$$\frac{dP}{dT} = s(g(N,P,A)+h(N,P,A))P - mP, \tag{2}$$

$$P(0), N(0) > 0 \tag{3}$$

wherein the growth of the prey is influenced by Allee effect (strong/ weak) and the predator is provided with additional food. Here $N(t)$, $P(t)$ respectively represent prey and predator population densities at time t. K and L (with $-K < L < K$) are the carrying capacity and Allee effect threshold of the prey population respectively. r is the intrinsic growth rate of the prey. The parameters s and m, respectively, stand for growth and death rates of the predator. A is the amount of additional food [42], $g(N,P,A)$, $h(N,P,A)$ are the functional responses of the predator towards the prey and additional food respectively. Here, the forms for $g(N,P,A)$, $h(N,P,A)$ are assumed to be

$$g(N,P,A) = \frac{cN}{a+\alpha\eta A+N}, \tag{4}$$

$$h(N,P,A) = \frac{c\eta A}{a+\alpha\eta A+N} \tag{5}$$

where c is the maximum rate of predation, a is the half saturation level of the functional response in the absence of additional food. η represents ability of the predator to detect the prey relative to predator and the term ηA stands for quantity of additional food perceptible by the predator relative to prey (effectual additional food level) and α represents the quality of additional food relative to prey [42]. In the absence of additional food, the functional response $g(N,P,A)$ reduces to the Holling type II functional response and $h(N,P,A)$ reduces to zero. With the functions (4), (5) and denoting $b = cs$, the model (1)–(2) takes the form

$$\frac{dN}{dT} = rN(N-L)\left(1-\frac{N}{K}\right) - \frac{cNP}{a+\alpha\eta A+N}, \tag{6}$$

$$\frac{dP}{dT} = \frac{b(N+\eta A)P}{a+\alpha\eta A+N} - mP. \tag{7}$$

To reduce the number of parameters, we introduce three dimensionless variables x, y and t, and five dimensionless parameters θ, γ, ξ, β and δ given by $x = \frac{N}{a}$, $y = \frac{cP}{ra^2}$, $t = arT$, $\theta = \frac{L}{a}$, $\gamma = \frac{K}{a}$, $\xi = \frac{\eta A}{a}$, $\beta = \frac{b}{ra}$ and $\delta = \frac{m}{ra}$, thereby reduce the system (6)–(7) to the form

$$\dot{x} = x(x-\theta)\left(1-\frac{x}{\gamma}\right) - \frac{xy}{1+\alpha\xi+x}, \tag{8}$$

$$\dot{y} = \frac{\beta(x+\xi)y}{1+\alpha\xi+x} - \delta y, \tag{9}$$

$$x(0) \equiv x_0 \geq 0,\ y(0) \equiv y_0 \geq 0 \tag{10}$$

All the parameters involved with the model are positive except θ. It is well known that the Allee effect is classified as strong Allee effect and weak Allee effect whenever the parameter θ satisfies $0 < \theta < \gamma$ and $\theta < 0$ respectively [40].
Defining

$$f(x) = \frac{x}{1+\alpha\xi+x},$$

$$g(x) = (1+\alpha\xi+x)(x-\theta)\left(1-\frac{x}{\gamma}\right),$$

the above predator-prey system (8)–(9) can be expressed as

$$\dot{x} = [g(x) - y]\, f(x), \tag{11}$$

$$\dot{y} = \left[\beta f(x)\left(1+\frac{\xi}{x}\right) - \delta\right] y. \tag{12}$$

For the predator-prey system (11)–(12), the prey nullclines are: y-axis, the curve $y = g(x)$ and the predator nullclines are: x-axis, the straight line $x = \frac{\delta(1+\alpha\xi)-\beta\xi}{\beta-\delta}$, which is a part of $\beta f(x)\left(1+\frac{\xi}{x}\right) - \delta = 0$ lying within the first quadrant. The prey nullcline $y = g(x)$ intersects the x-axis at $(\theta, 0)$, $(\gamma, 0)$ and $g(x)$ is positive in the interval (θ, γ). Also, the prey nullcline $y = g(x)$ has a hump at $x = x_H \in (\theta, \gamma)$ and it is increasing (*ie*, $g'(x) > 0$) in (θ, x_H) and decreasing (*ie*, $g'(x) < 0$) in (x_H, γ) where

$$x_H = \frac{1}{3}\left((\gamma+\theta) - -(1+\alpha\xi)\right) + \frac{1}{3}\left(\sqrt{[(\gamma+\theta) - -(1+\alpha\xi)]^2 + 3[(1+\alpha\xi)(\gamma+\theta) - \gamma\theta]}\right).$$

Thus, the prey nullcline $y = g(x)$ is negative in $(0, \theta)$ and positive in (θ, γ) in case of strong Allee effect whereas it is positive in $(0, \gamma)$ in case of weak Allee effect. The predator nullcline $x = \frac{\delta(1+\alpha\xi)-\beta\xi}{\beta-\delta}$ lies in the positive quadrant if $\delta(1+\alpha\xi) - \beta\xi$ and $\beta - \delta$ have the same sign.

3 Local stability and bifurcation

In this section we study the predator-prey system (11)–(12) to identify its equilibrium solutions, find their stability nature and provide local bifurcation analysis.

3.1 Existence of equilibria

First we find the number of equilibrium solutions admitted by the system (11)–(12) and investigate their local stability properties. We observe that the system (11)–(12) always admits the trivial equilibrium $E_0 = (0, 0)$ and the axial equilibrium point $E_\gamma = (\gamma, 0)$. It admits yet another axial equilibrium $E_\theta = (\theta, 0)$ if the Allee effect in the prey population is strong. Existence of interior equilibrium $E_* = (x_*, y_*)$, where

$$x_* = \frac{\delta(1+\alpha\xi) - \beta\xi}{\beta - \delta},$$

$$y_* = g(x_*) = (1+\alpha\xi+x_*)(x_*-\theta)\left(1-\frac{x_*}{\gamma}\right), \tag{13}$$

depends on the positivity of its components. Positivity of x_* is assured if one of the following conditions

$$\frac{\xi}{1+\alpha\xi} < \frac{\delta}{\beta} < 1, \tag{14}$$

$$\frac{\xi}{1+\alpha\xi} > \frac{\delta}{\beta} > 1 \tag{15}$$

is satisfied. Positivity of y_* is guaranteed if $\theta < x_* < \gamma$ in case of strong Allee effect and $0 < x_* < \gamma$ in case of weak Allee effect. Thus the considered system admits at least three and at most four equilibria incase of strong Allee effect and at least two and at most three equilibria in case of weak Allee effect.

In view of the above discussion we can conclude that, whenever the parameters satisfy either (14) or (15) and $x_* < \gamma$, the system (11)–(12) admits a unique interior equilibrium if either

$$\theta(\beta - \delta) < \delta(1+\alpha\xi) - \beta\xi < \gamma(\beta - \delta), \tag{16}$$

or

$$0 < \delta(1+\alpha\xi) - \beta\xi < \gamma(\beta - \delta), \tag{17}$$

are satisfied in the cases of strong or weak Allee effect respectively.

3.2 Local stability analysis

Having identified the equilibrium solutions of the considered system (11)–(12), we evaluate the local stability nature of each of the equilibrium solutions. This enables us to understand the nonlinear dynamics associated with the system by investigating the involved local and global bifurcations. In order to study the bifurcations we concentrate on two parameters of the system given by θ, the strength of the Allee effect and δ, the death rate of the predator. Variations in

Table 1 Table presenting the existence, eigenvalues of the Jacobian matrix (18) and stability nature at the concerned equilibrium point for the prey-predator system (11)–(12) with weak Allee effect (WAE) and strong Allee effect (SAE)

Equilibrium point	Existence		Eigenvalues of the Jacobian	Nature of equilibrium	
	WAE	SAE		WAE	SAE
$E_0 = (0, 0)$	Exists	Exists	$-\theta, \delta_0 - \delta$	Unstable node if $\delta < \delta_0$Saddle if $\delta > \delta_0$	Saddle if $\delta < \delta_0$Stable if $\delta > \delta_0$
$E_\theta = (\theta, 0)$	Does not exist	Exists	$\frac{\theta}{\gamma}(\gamma - \theta), \delta_{T_\theta} - \delta$		Unstable node if $\delta < \delta_{T_\theta}$Saddle if $\delta > \delta_{T_\theta}$
$E_\gamma = (\gamma, 0)$	Exists	Exists	$\theta - \gamma, \delta_{T_\gamma} - \delta$	Saddle if $\delta < \delta_{T_\gamma}$ stable if $\delta > \delta_{T_\gamma}$	Saddle if $\delta < \delta_{T_\gamma}$ stable if $\delta > \delta_{T_\gamma}$
$E_* = (x_*, y_*)$	Exists if $0 < x_* < \gamma$	Exists if $\theta < x_* < \gamma$	Roots of characteristic equation of the Jacobian matrix (18)	Unstable if $\delta \in (\delta_0, \delta_H)$ and $\delta_0 < \delta < \beta$Stable if $\delta \in (\delta_H, \delta_{T_\gamma})$ and $\delta_0 < \delta < \beta$Saddle if $\delta \in (\delta_0, \delta_{T_\gamma})$ and $\beta < \delta < \delta_0$	Unstable if $\delta \in (\delta_{T_\theta}, \delta_H)$ and $\delta_0 < \delta < \beta$Stable if $\delta \in (\delta_H, \delta_{T_\gamma})$ and $\delta_0 < \delta < \beta$Saddle if $\delta \in (\delta_{T_\theta}, \delta_{T_\gamma})$ and $\beta < \delta < \delta_0$

the parameter θ facilitates a comparative study in the system dynamics with respect to the strength of the Allee effect. Study associated with variations in the parameter δ highlights dependance of the system dynamics on the death rate of the predators and also indicates the consequences of linear proportionate harvesting in predator population. Thus we derive the Jacobian matrix of the system (11)–(12) through the standard process of linearization and analyse its eigenvalues to identify the nature of the associated equilibrium point. The general form of the Jacobian matrix of the considered system (11)–(12) at any point (x, y) is given by

$$J(x, y) = \begin{pmatrix} g'(x)f(x) + [g(x) - y]f'(x) & -f(x) \\ \beta y\left[f'(x)\left(1 + \frac{\xi}{x}\right) - \frac{f(x)}{x^2}\xi\right] & \beta f(x)\left(1 + \frac{\xi}{x}\right) - \delta \end{pmatrix} \tag{18}$$

where

$$f'(x) = \frac{1 + \alpha\xi}{(1 + \alpha\xi + x)^2},$$
$$g'(x) = -\frac{3}{\gamma}x^2 + 2\left[\left(1 + \frac{\theta}{\gamma}\right) - \frac{1}{\gamma}(1 + \alpha\xi)\right]x + \left[(1 + \alpha\xi)\left(1 + \frac{\theta}{\gamma}\right) - \theta\right].$$

Evaluating the Jacobian $J(x, y)$ at each of the equilibrium solutions we come across four critical values for the parameter δ given by $\delta_0 = \frac{\beta\xi}{1+\alpha\xi}$, $\delta_{T_\theta} = \frac{\beta(\theta+\xi)}{1+\alpha\xi+\theta}$, $\delta_{T_\gamma} = \frac{\beta(\gamma+\xi)}{1+\alpha\xi+\gamma}$ and $\delta_H = \frac{\beta(x_H+\xi)}{1+\alpha\xi+x_H}$. Significance of these critical values is presented in Table 1.

From Table 1 we clearly understand that the system undergoes trans-critical bifurcation at the equilibria E_θ, E_γ (if admitted by the system) whenever the parameter δ equals δ_{T_θ}, δ_{T_γ} respectively and Hopf-bifurcation occurs around E_* whenever $\delta = \delta_H$, provided the parameters satisfy the condition (14). No Hopf bifurcation can occur at E_* if the parameters follow the condition (15), in which case E_* remains as a saddle point throughout. Below we give theoretical support for the occurrence of foresaid bifurcations.

3.3 Transcritical bifurcations

The expressions for the eigenvalues presented in Table 1 and the corresponding stability nature associated with the axial equilibria clearly indicate the occurrence of transcritical bifurcation at the equilibrium E_γ which is independent of sign of θ and also at E_θ for the case of strong Allee effect. An application of Sotomayer theorem (See "Appendix") confirms the occurrence of transcritical bifurcation at E_γ and E_θ when $\delta = \delta_{T_\gamma}$ and $\delta = \delta_{T_\theta}$ respectively.

The interior equilibrium emerged or annihilated due to occurrence of two transcritical bifurcations at the axial equilibria E_θ and E_γ respectively and the respective bifurcation conditions are given by (14) and (15). These two transcritical bifurcation curves are shown in the bifurcation diagrams presented in Figs. 1 and 4.

3.4 Hopf bifurcation

Let J_* represent the Jacobian matrix evaluated at E_*. It can be easily verified that

$$Tr(J_*) = g'(x_*)f(x_*) \tag{19}$$

and

$$Det(J_*) = \beta g(x_*)f(x_*)\left[f'(x_*)(1 + \frac{\xi}{x_*}) - \frac{f(x_*)}{x_*^2}\xi\right] = \frac{\beta g(x_*)f(x_*)}{(1 + \alpha\xi + x_*)^2}[1 + \alpha\xi - \xi]. \tag{20}$$

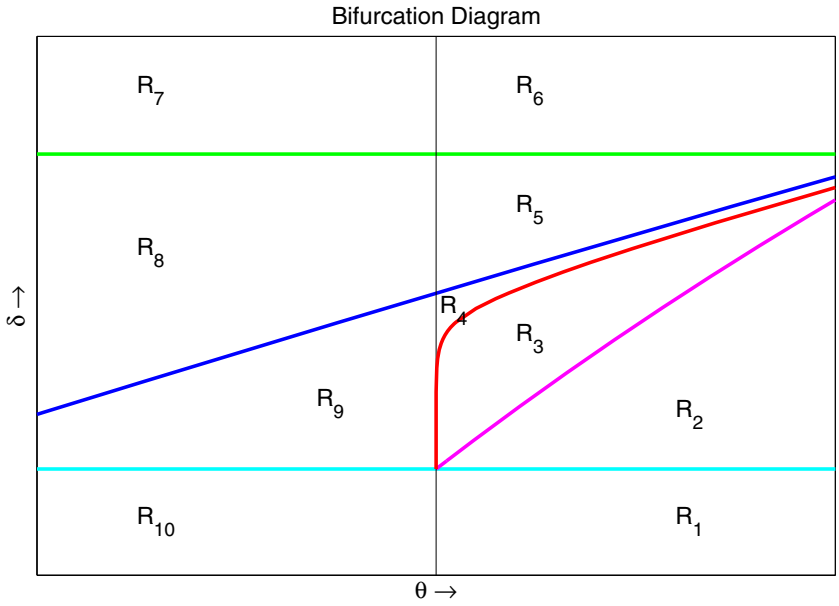

Fig. 1 Figure presenting the bifurcation diagram in the upper half plane of (θ, δ) space for the case where parameters of the model (11)–(12) satisfy the condition (14). The *curve in cyon* represents (21). The transcritical bifurcation curve at E_θ (22) is represented by the *magenta curve*. The *green curve* represents transcritical bifurcation curve at E_γ (23). The *blue curve* represents Hopf bifurcation curve (24) at E_*. The curve presented in *red colour* represents occurrence of heteroclinic bifurcation between the two saddles E_θ and E_γ. (Color figure online)

Clearly, Hopf bifurcation can not occur at E_* under the assumption (15), as it remains a saddle due to negativity of $Det(J_*)$. Now, let us assume that the parameters satisfy the condition (14). Here we have $Det(J_*)$ to be positive and $Tr(J_*)|_{\delta=\delta_H} = f(x_H)g'(x_H) = 0$ (since $x_* = x_H$ whenever $\delta = \delta_H$). Differentiating trace of J_* with respect to the bifurcation parameter δ, we obtain

$$\begin{aligned}\frac{d}{d\delta}(Tr(J_*)) &= f'(x_*)g'(x_*)\frac{dx_*}{d\delta} + f(x_*)g''(x_*)\frac{dx_*}{d\delta}\\ &= \left(f'(x_*)g'(x_*)+f(x_*)g''(x_*)\right)(1+\alpha\xi+x_*).\end{aligned}$$

Therefore

$$\begin{aligned}&\frac{d}{d\delta}(Tr(J_*))\,|_{\delta=\delta_H}\\ &= \left(f'(x_H)g'(x_H) + f(x_H)g''(x_H)\right)(1+\alpha\xi+x_H)\\ &= \frac{2x_H}{\gamma}\left(\sqrt{[(\gamma+\theta)-(1+\alpha\xi)]^2+3[(1+\alpha\xi)(\gamma+\theta)-\gamma\theta]}\right).\end{aligned}$$

Thus we have $\frac{d}{d\delta}(Tr(J_*))\,|_{\delta=\delta_H} > 0$. Hence the transversality condition for Hopf bifurcation is satisfied. The stability of the Hopf bifurcating limit cycle is determined by the first Lyapunov coefficient and we are not providing its expression here from the sake of brevity [46]. Numerically we have verified that the limit cycles are stable whenever they exist. Thus the considered system (11)–(12) undergoes a supercritical Hopf bifurcation at $\delta = \delta_H$ whenever the parameters satisfy the condition (14) and this is independent of sign of θ. Here, we see that lowering δ gives an increasing period of the limit cycle that arises through the Hopf-bifurcation. This Hopf-bifurcation curve ($\delta = \delta_H$) is represented by the blue curve in Fig. 1. In case of strong Allee effect, the limit cycle, that appears through Hopf bifurcation, increase in size (as the predator isocline crosses the hump of the prey isocline and moves closer to y-axis) until it disappears through the heteroclinic bifurcation. At the heteroclinic bifurcation threshold we find the heteroclinic cycle joining the saddle points E_θ and E_γ. The curve on which the limit cycle disappears is represented by the red curve in Fig. 1.

4 Global dynamics

Information on the number of equilibrium solutions admitted by the system, the nature of the equilibria and the local bifurcations at equilibrium points identify the following four significant relations between the system parameters using which the global dynamics of the system can be determined.

$$h_1(\theta,\delta) \equiv \beta\xi - \delta(1+\alpha\xi) = 0, \tag{21}$$

$$h_2(\theta,\delta) \equiv \beta(\theta+\xi) - \delta(1+\alpha\xi+\theta) = 0, \tag{22}$$

$$h_3(\theta,\delta) \equiv \beta(\gamma+\xi) - \delta(1+\alpha\xi+\gamma) = 0 \tag{23}$$

and

$$h_4(\theta,\delta) \equiv g'(x_*) = g'\left(\frac{\delta(1+\alpha\xi)-\beta\xi}{\beta-\delta}\right) = 0. \tag{24}$$

Observe that the above curves represent occurrence of transcritical bifurcation at E_0, E_θ, E_γ and Hopf-bifurcation at E_* respectively. Since we assumed θ and δ to be bifurcation parameters, we plot the above curves in the upper half plane of (θ, δ) space for fixed parameter values of γ, α, ξ and β. Here we obtain two distinct bifurcation diagrams (Figs. 1, 4) corresponding to the parametric restrictions

satisfying the conditions (14) and (15) respectively. Apart from the curves (21)–(24), Fig. 1 presents yet another curve (shown in red colour) that signifies the occurrence of saddle-saddle connection in the phase space. Thus, there are five curves in Fig. 1 and three in Fig. 4. In both these figures, the first and second quadrants respectively represent the system bifurcations associated with strong and weak Allee effects respectively.

Note that the curves presented in each of the Figs. 1 and 4 divide the two quadrants into finite number of subregions. These subregions characterise nature of the equilibria admitted by the system. Observe that there are ten such regions (six for strong Allee effect and four for weak Allee effect) in Fig. 1 and seven such regions (four for strong Allee effect and three for weak Allee effect) in Fig. 4. Below we shall discuss the global dynamics of the system as the bifurcation parameters move through each of these regions.

Let us consider the bifurcation diagram presented in Fig. 1. In the case of strong Allee effect, we start with a small value of δ lying in the region R_1. In this region we have $h_1(\theta, \delta) < 0$, $h_2(\theta, \delta) > 0$ and $h_3(\theta, \delta) > 0$ meaning that E_0 is saddle, E_θ is unstable node and E_γ is saddle point respectively and hence all the solutions starting in this region exhibit blow up in the predator component (see phase portraits for Region R_1 in Fig. 2). Essentially the region R_1 represents the situation where the predator nullcline lies in the second quadrant of the phase space. As we move from R_1 to R_2 we have $h_1(\theta, \delta) > 0$, $h_2(\theta, \delta) > 0$ and $h_3(\theta, \delta) > 0$ indicating that E_0 is stable, E_θ is unstable node and E_γ is saddle point respectively. Thus the predator and prey population always tend to extinction. Therefore E_0 is globally asymptotically stable (see phase portraits for Region R_2 in Fig. 2).

As we enter R_3 from R_2 we have emergence of the interior equilibrium point E_*. In this region we have $h_2(\theta, \delta) < 0$ and $h_4(\theta, \delta) > 0$. Hence we have E_θ to be saddle point and the interior equilibrium point E_* to be unstable node. The transcritical bifurcation taking place due to exchange of stability between E_θ and E_* along the curve (23) that separates the region R_2 and R_3. The nature of the equilibrium points E_0 and E_γ remains unchanged. E_0 being the only asymptotically stable equilibrium, all the non equilibrium solutions initiating in the positive quadrant of the phase space approach E_0 asymptotically leading to eventual extinction of both predator and prey population (see phase portraits for Region R_3 in Fig. 2).

As we enter the region R_4 from R_3 the interior equilibrium point E_* turns into unstable focus from unstable node and the stability nature of all other equilibria remains unchanged. The heteroclinic orbit (green colour path), joining the two saddle points E_θ and E_γ, that occurs along the boundary curve between R_4 and R_3 is presented in the bifurcation diagram (see Heteroclinic, Fig. 2). Since this saddle-saddle connection is broken in R_4, the stable manifold of E_θ divides the phase plane into two invariant sub regions such that one of them contains E_0 and the other contains E_* and E_γ. All the paths with their initial state present in the region containing E_0 will eventually reach E_0 and those initiating in the region containing E_* and E_γ approach a stable limit cycle surrounding the unstable focus E_* (see phase portraits for Region R_4 in Fig. 2). Therefore co-existence or extinction of population depends on the initial state of the system. As we move from R_4 to R_5 we have $h_4(\theta, \delta) < 0$ and hence the interior equilibrium E_* becomes asymptotically stable while the stability nature of the axial equilibria E_0, E_θ and E_γ remain unchanged. Here the separatrix (stable manifold of E_θ) marks the boundary between the basins of attraction of the two asymptotically stable equilibria E_0 and E_*. Depending on the initial state in the basins of attraction, the trajectories of the system either tend to E_0 or to E_*. So, either the predator and prey go to extinction or there is stable coexistence between the prey and the predator (see phase portraits for Region R_5 in Fig. 2). Thus as we move from R_5 to R_4, the limit cycles that appear due to hopf bifurcation occurring along the curve $h_4(\theta, \delta) = 0$ increase in size until they disappear when the heteroclinic curve joining the points E_θ and E_γ is broken, which occurs on the boundary between R_4 and R_3.

As we enter the region R_6 from R_5 we have occurrence of transcritical bifurcation at E_γ leading to exchange of stability between E_* and E_γ and disappearance of E_*. The system admits two asymptotically stable equilibria E_0 and E_γ whose basins of attraction are separated by the stable manifold of the saddle point E_θ. Hence, the eventual state of the system (E_0 or E_γ) depends on the initial state. Irrespective of the initial state, the predators get extinct where as the prey population either survives and reaches its carrying capacity or gets extinct (see phase portraits for Region R_6 in Fig. 2).

So far we have discussed the global dynamics of the considered system (11)–(12) under the influence of strong Allee effect with the assumption that the parameters satisfy the condition (14). Now let us look at the bifurcation diagram for the case of weak Allee effect which is represented by the second quadrant in the Fig. 1. In region R_7, we have that $h_1(\theta, \delta) < 0$ and $h_3(\theta, \delta) < 0$ meaning that E_0 is saddle and E_γ is asymptotically stable (see phase portraits for Region R_7 in Fig. 3). Hence all the solutions initiating in the positive quadrant eventually approach E_γ making it globally asymptotically stable. As we enter R_8 from R_7 through the curve $h_3(\theta, \delta) = 0$, transcritical bifurcation takes place at E_γ leading to exchange of stability between E_γ and the newly emerged interior equilibrium E^*. Since $h_3(\theta, \delta) > 0$ and $h_4(\theta, \delta) < 0$ we have E_γ to be saddle point and the interior equilibrium point E_* to be asymptotically stable node (see phase portrait for Region R_8 in Fig. 3). Thus, in the region R_8, E_* is globally asymptotically stable. As we move

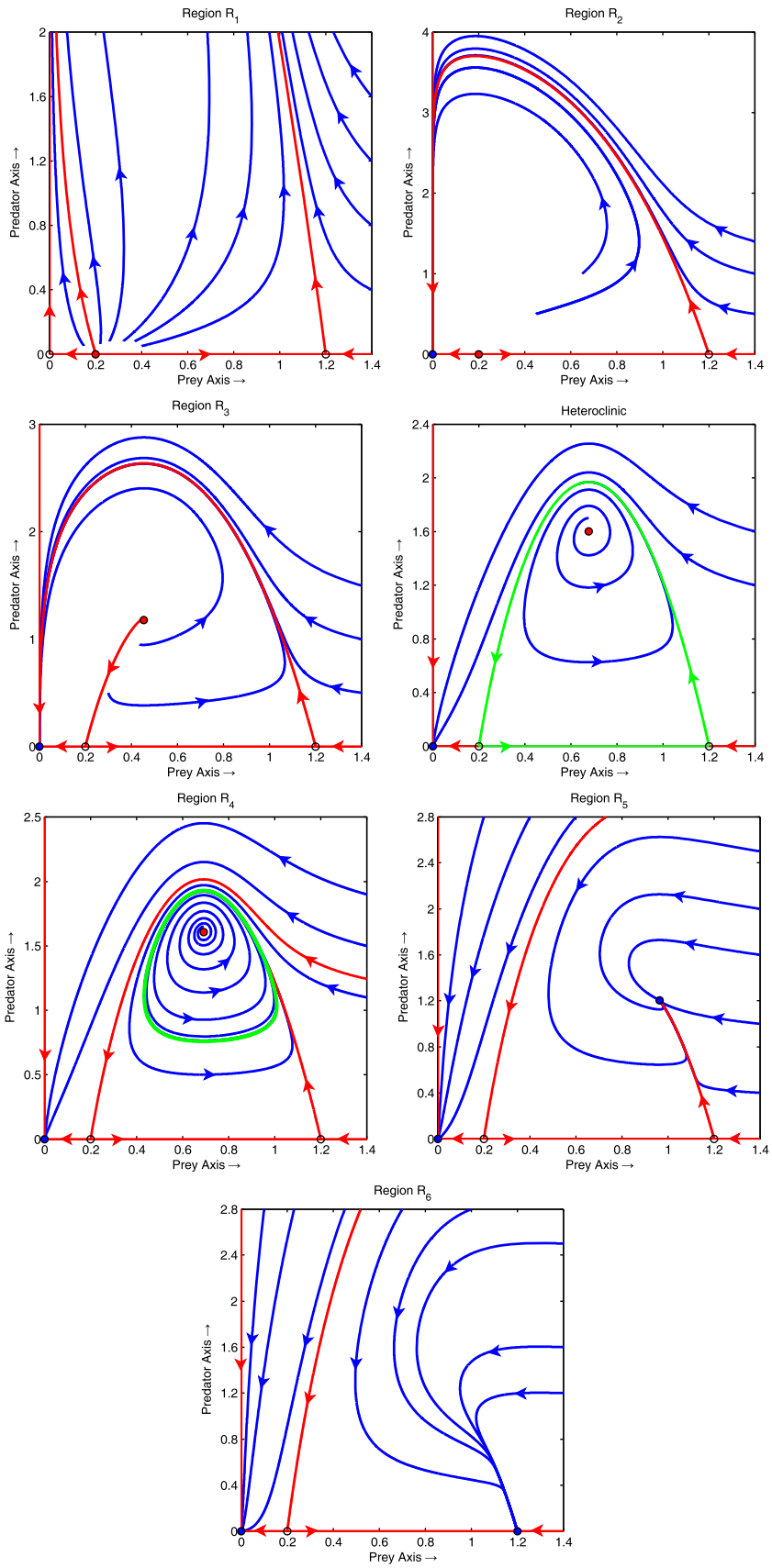

Fig. 2 Phase portraits of the considered system (11)–(12) satisfying (14) with strong Allee effect for different values of δ. $\delta = 0.25$ (Region R_1), $\delta = 0.55$ (Region R_2), $\delta = 0.62$ (Region R_3), $\delta = 0.6746878728994055$ (Heteroclinic), $\delta = 0.678$ (Region R_4), $\delta = 0.74$ (Region R_5), $\delta = 0.81$ (Region R_6). Here $\theta = 0.2$, $\gamma = 1.2$, $\alpha = 4.3$, $\xi = 1.4$ and $\beta = 2.5$ are fixed parameters

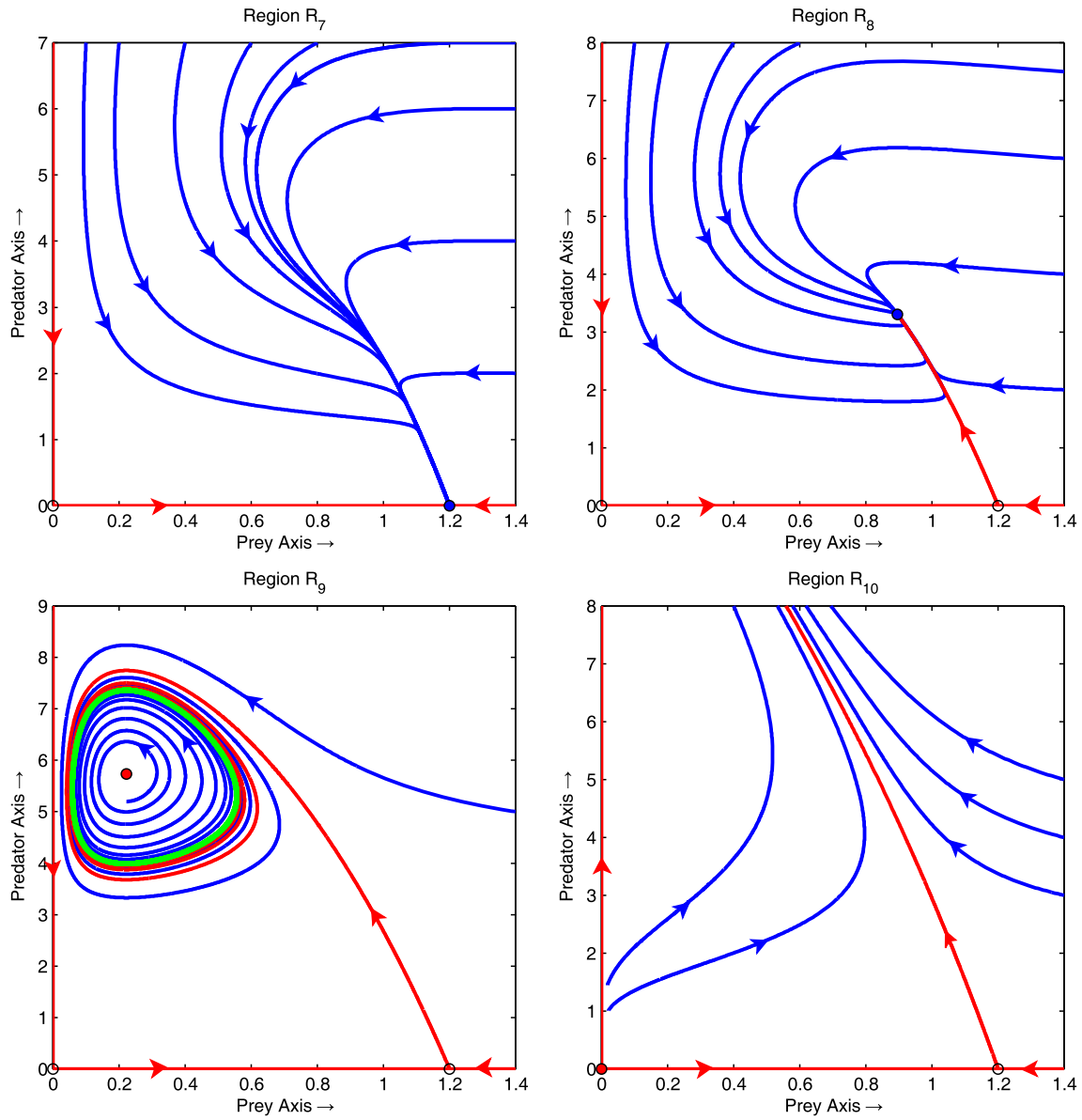

Fig. 3 Phase portraits of the considered system (11)–(12) with weak Allee effect for different values of $\delta = 0.81$ (Region R_7), $\delta = 0.725$ (Region R_8), $\delta = 0.66$ (Region R_9), $\delta = 0.4$ (Region R_{10}). Here $\theta = -0.75$, $\gamma = 1.2$, $\alpha = 4.3$, $\xi = 1.4$ and $\beta = 2.5$ are fixed parameters

from R_8 to R_9 we have $h_4(\theta, \delta) > 0$ and hence the interior equilibrium point E_* is unstable focus surrounded by a limit cycle while the stability of other equilibrium points remains unchanged. Therefore both the predators and prey asymptotically approach the stable limit cycle surrounding the unstable focus (see phase portrait for Region R_9 in Fig. 3). This is due to the occurrence of Hopf-bifurcation along the curve $h_4(\theta, \delta) = 0$. Here the limit cycle surrounding E_* is the global attractor. Moving from R_9 to R_{10} we have $h_1(\theta, \delta) > 0$ and hence E_0 becomes unstable and the interior equilibrium disappears. The saddle nature of the axial equilibrium E_γ remains unchanged. Therefore all solutions starting in the first quadrant blow up in the $y-$direction (see phase portraits for Region R_{10} in Fig. 3).

So far, we described the bifurcation diagram (Fig. 1) in greater detail by using phase portraits that give better understanding of the dynamical behavior of the considered model (11)–(12). The phase portraits corresponding to the different regions of the bifurcation diagram (Fig. 1) for strong Allee effect ($R_1 - R_6$) and weak Allee effect ($R_7 - R_{10}$) are presented in Figs. 2, 3 respectively. The values of the parameters are mentioned in the captions of the respective figures. In these phase portraits, the saddle, stable, unstable equilibrium points are represented by circles, circles filled with blue color and circles filled with red color respectively. Stable and unstable manifolds are represented by red curves. Limit cycles are represented in green and paths are represented in blue.

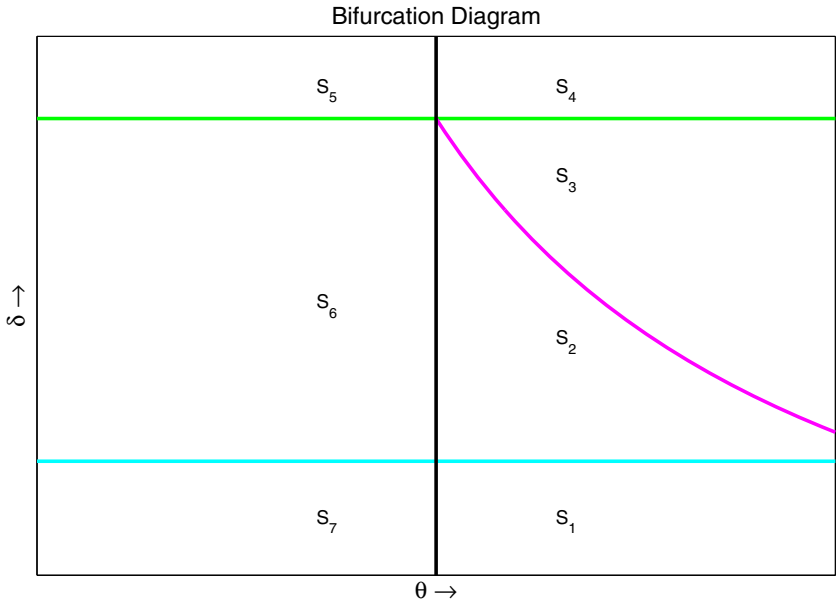

Fig. 4 Figure presenting the bifurcation diagram in the upper half plane of (θ, δ) space for the case where parameters of the model (11)–(12) satisfying (15). The *curve in cyon* represents (21). The transcritical bifurcation curve at E_θ (22) is represented by the *magenta curve*. The *green curve* represents transcritical bifurcation curve at E_γ (23). (Color figure online)

Now Fig. 5 presents another bifurcation diagram (in (x, δ) plane) that depicts the stability nature of the equilibria of the considered model (11)–(12) with strong Allee effect under the parametric condition (14). The three blue color dotted vertical lines $\delta = \delta_{T_\theta}, \delta = \delta_H$ and $\delta = \delta_{T_\gamma}$ represent transcritical bifurcation at E_θ, Hopf-bifurcation at $(x_H, g(x_H))$ and transcritical bifurcation at E_γ respectively. The heteroclinic orbit, connecting the two saddle points E_θ and E_γ comes into existence at $\delta = \delta_{Het}$. The axial equilibrium points always exist and E_0 is asymptotically stable represented by solid magenta line, E_θ is unstable (saddle) if $\delta < \delta_{T_\theta}$ $(\delta > \delta_{T_\theta})$ and E_γ is saddle (stable) if $\delta < \delta_{T_\gamma}$ $(\delta > \delta_{T_\gamma})$. The interior equilibrium point exists for $\delta \in (\delta_{T_\theta}, \delta_{T_\gamma})$ but it is unstable node for $\delta \in (\delta_{T_\theta}, \delta_{Het})$, unstable focus for $\delta \in (\delta_{Het}, \delta_H)$ and locally asymptotically stable for $\delta \in (\delta_H, \delta_{T_\gamma})$. Red color dotted line represents the x component of the unstable interior equilibrium point. The x component of the stable interior equilibrium point along with the minimum and maximum of the stable limit cycle surrounding an unstable focus is presented (red in color). One can easily observe the existence of bistability in the system for $\delta > \delta_{Het}$ for the considered model (11)–(12) with strong Allee effect. Similarly, Fig. (6) presents the bifurcation diagram for the system (11)–(12) with weak Allee effect when the involved parameters satisfy the condition (14).

Now, let us look at the other case where parameters of the system follow the condition (15). Bifurcation diagram corresponding to this case is represented in Fig. 4 which presents division of parameter space into seven regions. The phase portraits of the system (11)–(12) corresponding to the subregions depicted in Fig. 4 are presented in the Figs. 7 and 8. The description pertaining to the bifurcation diagram and the corresponding phase portraits can be presented in a similar as in the previous case.

5 Discussion

Growing importance for eco-friendly practices for managing and controlling ecosystems has driven experimental scientists to perform various experiments to identify appropriate methods for biological control. One of the established methods happens to be provision of additional food to predators. This method is expected to enhance the survival of the predators in the environment. Further, it is anticipated that the increased growth in predators would control and limit the resident prey (pest). On the contrary, it is observed that provision of additional food to predators did not always increase the population density of the predators. There were occasions where this provision lead to decrease in predators and increase in the pest density. This contra intuitive observation has motivated the theoretical scientists to investigate into the influence of additional food on the dynamics of interacting species such as predator-prey systems in order to offer explanation for the observations made by experimental scientists. Recent studies [42–45] not only highlight the necessity for undertaking such studies but also provide state of art in this area.

In this article we study the dynamics of a predator-prey system when the predator is provided with additional food and the prey growth is influenced by Allee effect. The considered model takes both strong and weak Allee effects into consideration. Analysis of the system highlights the bifurcations associated with the dynamics. It is observed that inclusion of additional food into the system enriches

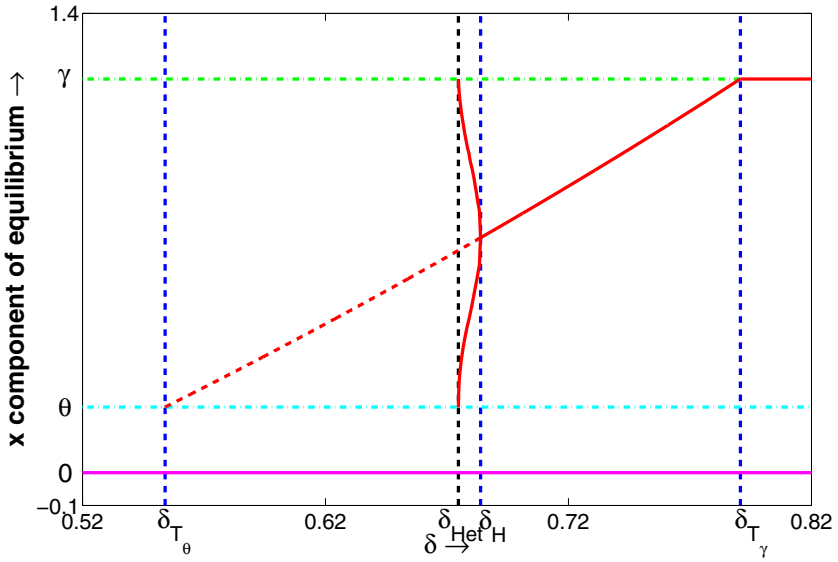

Fig. 5 Figure presenting the bifurcation diagram for stability of equilibrium point of the considered model with strong Allee effect under the parametric conditions (14). E_0 is stable and E_θ is unstable for $\delta \in [0.52, 0.82]$. E_γ is unstable for $\delta \in [0.52, \delta_{T_\gamma})$ and stable for $\delta \in (\delta_{T_\gamma}, 0.82]$, E_γ and E_* coincides at the transcritical bifurcation threshold δ_{T_γ}. Interior equilibrium point E_* is feasible for $\delta_{T_\theta} < \delta < \delta_{T_\gamma}$ and is stable for $\delta_H < \delta < \delta_{T_\gamma}$. E_* loses stability through super-critical Hopf-bifurcation at δ_H and stable limit cycle exists for $\delta_{\text{Het}} < \delta < \delta_H$. The stable limit cycle disappear through a heteroclinic bifurcation and heteroclinic loop is formed by joining two axial equilibrium points E_θ and E_γ

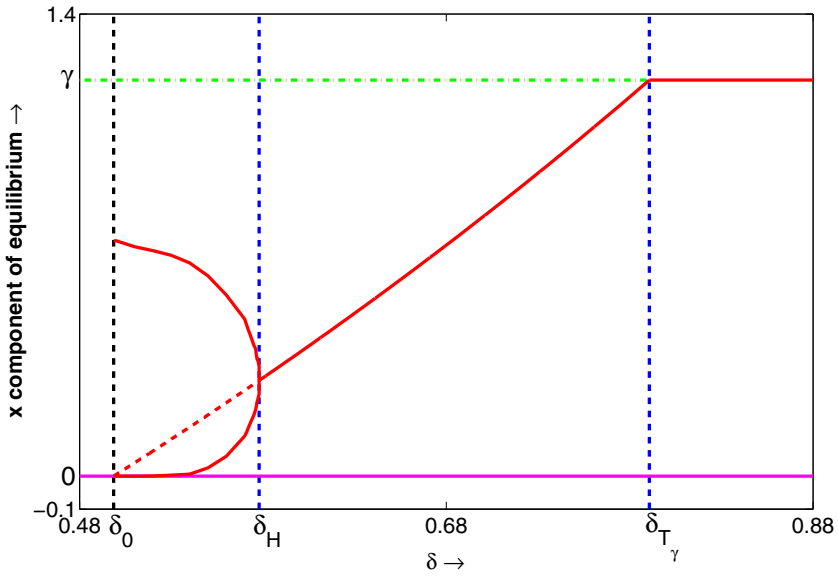

Fig. 6 Figure presenting the bifurcation diagram for stability of equilibrium point of the considered model with weak Allee effect where the parameters of the system satisfying (14). E_0 is stable for $\delta \in [0.48, 0.88]$ and E_γ is stable for $\delta \in (\delta_{T_\gamma}, 0.88]$. E_γ and E_* coincide with each other at the transcritical bifurcation threshold δ_{T_γ}. Interior equilibrium point E_* is feasible for $\delta_{T_\theta} < \delta < \delta_0$ and is stable for $\delta_H < \delta < \delta_{T_\gamma}$. E_* loses stability through super-critical Hopf-bifurcation at δ_H and stable limit cycle exists for $\delta_0 < \delta < \delta_H$

the system dynamics. This analysis also offers strategies to manipulate the additional food provision for accomplishing the desired results in the system such as elimination of prey from the system (an application to pest management) or distraction of predators from prey (an application to biological conservation) there by enhance chances of survival for prey.

While provision of additional food to predators does not eliminate the characteristic features of the existing Allee effect in the system, it does affect the level of coexistence of the species considerably. The existence of interior equilibrium and variation in its stability behaviour much depends on the measure of a specific combination of quality and quantity of the additional food relative to unity as well as the ratio between the maximum growth rate and death rate of the predators. If the maximum growth rate of the predators is higher than their natural death rate then, with the quality and quantity of the additional food satisfying certain relations, it is possible to bring in coexistence of the species (if it is not

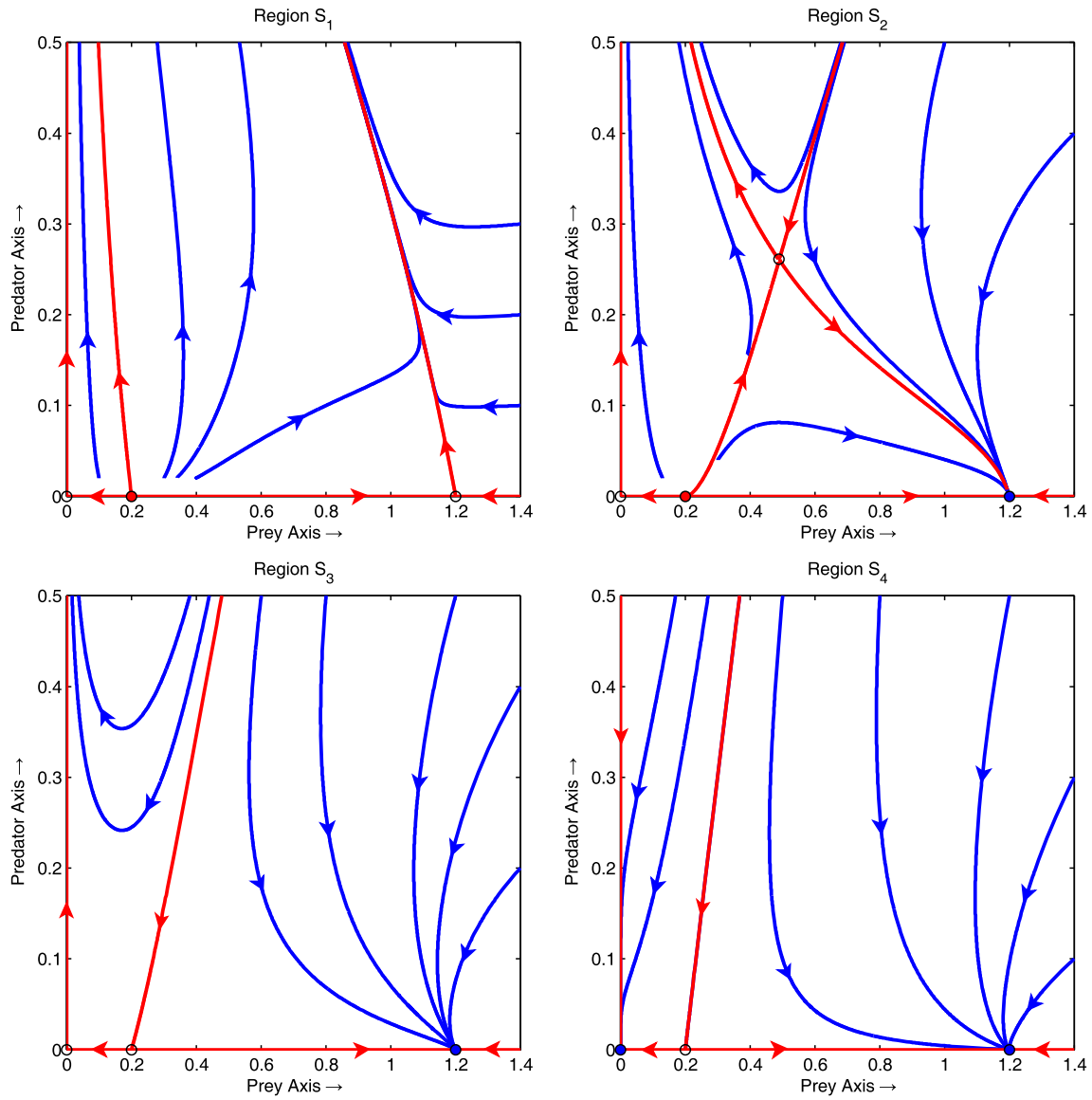

Fig. 7 Phase portraits of the considered system (11)–(12) with strong Allee effect for different values of $\delta = 1.80$ (Region S_1), $\delta = 2.2$ (Region S_2), $\delta = 2.52$ (Region S_3), $\delta = 2.824$ (Region S_4). Here $\theta = 0.2$, $\gamma = 1.2$, $\alpha = 0.01$, $\xi = 2.85$ and $\beta = 1$ are fixed parameters

originally present), alter the stability nature of the interior equilibrium and even eliminate the coexistence by changing the quality and quantity of additional food provided to predators.

On the other hand, if the maximum growth rate of the predators is lower than their natural death rate then although an interior equilibrium can be brought in (only in the case of strong Allee effect) through provision of additional food to predators, for all practical purposes co-existence of the species can not be achieved due to saddle nature of the interior equilibrium which can not be altered with variations in quality and quantity of additional food. As a result the system experiences either unlimited growth in the predator combined with prey extinction or asymptotic approach of the prey population to its carrying capacity along with extinction of predator population. Various regions presented in the bifurcation diagrams and the associated phase portraits can be used as the guiding principles for achieving the needed biological control results.

6 Appendix

Let $\boldsymbol{f}(x, y; \delta)$ represent the vector

$$\boldsymbol{f}(x, y; \delta) = \begin{pmatrix} x(x-\theta)(1-\frac{x}{\gamma}) - \frac{xy}{1+\alpha\xi+x} \\ \frac{\beta(x+\xi)y}{1+\alpha\xi+\gamma} - \delta y \end{pmatrix}. \tag{25}$$

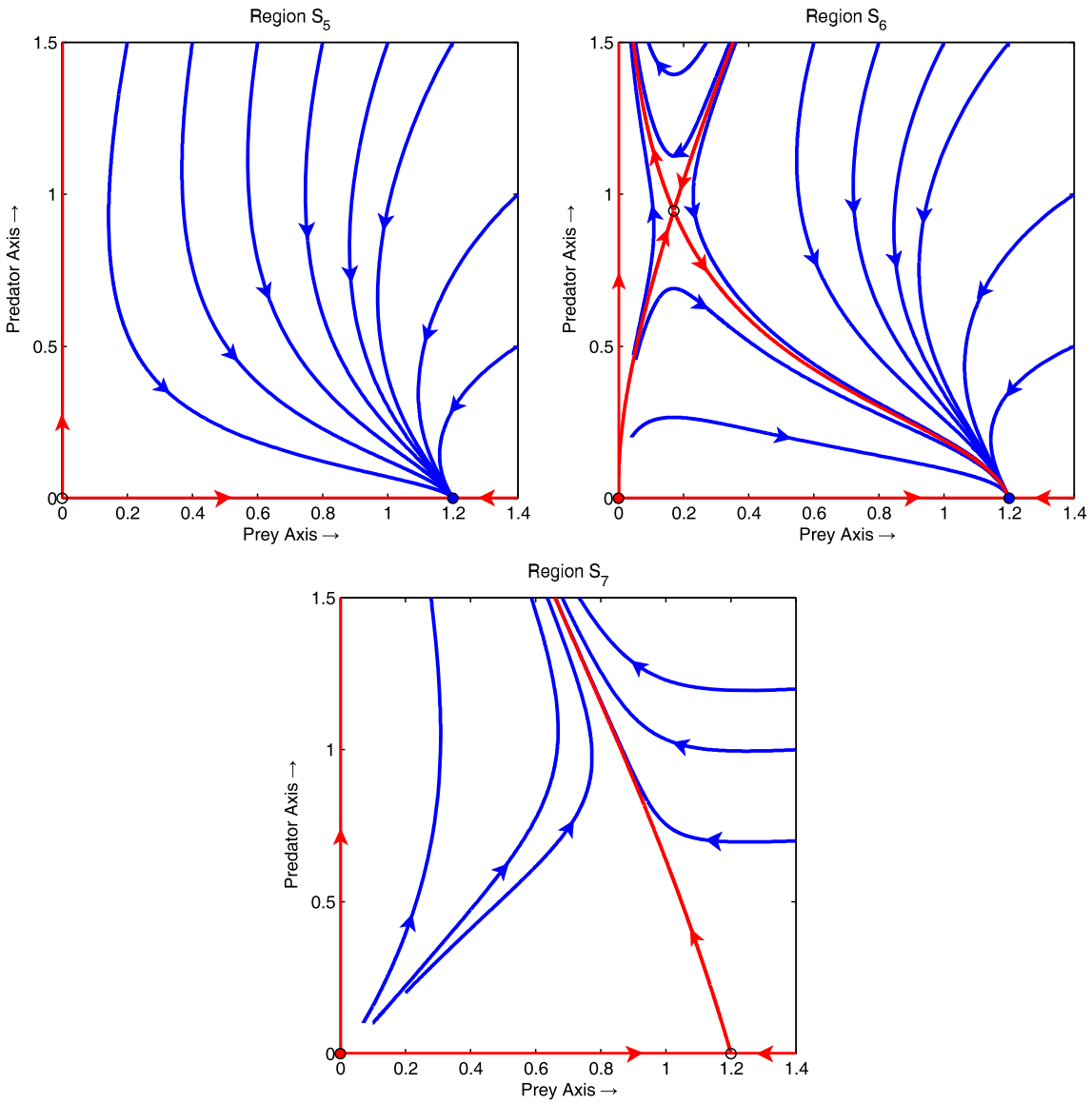

Fig. 8 Phase portraits of the considered system (11)–(12) with weak Allee effect for different values of $\delta = 2.82$ (Region S_5), $\delta = 2.52$ (Region S_6), $\delta = 1.80$ (Region S_7). Here $\theta = -0.75$, $\gamma = 1.2$, $\alpha = 0.01$, $\xi = 2.85$ and $\beta = 1$ are fixed parameters

Differentiate the above function with respect to δ, we obtain

$$\boldsymbol{f}_{\delta}(x, y; \delta) = \begin{pmatrix} 0 \\ -y \end{pmatrix}. \tag{26}$$

The jacobian matrix of the prey-predator system (8)–(9) at the equilibrium point E_θ is given by

$$P = J_1(\theta, 0) = \begin{pmatrix} \frac{\theta}{\gamma}(\gamma - \theta) & -\frac{\theta}{1+\alpha\xi+\theta} \\ 0 & \frac{\beta(\theta+\xi)}{1+\alpha\xi+\theta} - \delta \end{pmatrix}.$$

Observe that the Jacobian matrix P has a simple zero eigen values as its determinant is zero and the trace is different from zero whenever $x_* = \theta$. Let $\mathbf{v} = \begin{pmatrix} v_1 \\ v_2 \end{pmatrix}$ be an eigen vector of the Jacobian matrix P corresponding to the eigen value $\lambda = 0$. We have

$$P\mathbf{v} = \begin{pmatrix} \frac{\theta}{\gamma}(\gamma - \theta) & -\frac{\theta}{1+\alpha\xi+\theta} \\ 0 & 0 \end{pmatrix} \begin{pmatrix} v_1 \\ v_2 \end{pmatrix} = \begin{pmatrix} \frac{\theta}{\gamma}(\gamma - \theta) & v_1 - \frac{\theta v_2}{1+\alpha\xi+\theta} \\ & 0 \end{pmatrix}$$

and

$$\lambda\mathbf{v} = \begin{pmatrix} \lambda v_1 \\ \lambda v_2 \end{pmatrix} = \begin{pmatrix} 0 \\ 0 \end{pmatrix}.$$

We know that the vector $\mathbf{v}$ will be an eigen vector of P corresponding to the eigen value $\lambda = 0$ if $P\mathbf{v} = \lambda\mathbf{v}$. Clearly the components of this eigen vector satisfy the equation

$$\frac{\theta}{\gamma}(\gamma-\theta)v_1 - \frac{\theta v_2}{1+\alpha\xi+\theta} = 0$$

By choosing $v_1 = 1$ we obtain an eigen vector for P given by

$$\mathbf{v} = \begin{pmatrix} 1 \\ \frac{(\gamma-\theta)(1+\alpha\xi+\theta)}{\gamma} \end{pmatrix}. \tag{27}$$

Now, let $\mathbf{w} = \begin{pmatrix} w_1 \\ w_2 \end{pmatrix}$ be the eigen vector of the matrix $P^\top$ then

$$P^\top = \begin{pmatrix} \frac{\theta}{\gamma}(\gamma-\theta) & 0 \\ \frac{\theta}{1+\alpha\xi+\theta} & 0 \end{pmatrix}\begin{pmatrix} w_1 \\ w_2 \end{pmatrix} = \begin{pmatrix} \frac{\theta}{\gamma}(\gamma-\theta)w_1 \\ \frac{\theta w_1}{1+\alpha\xi+\theta} \end{pmatrix}$$

and

$$\lambda\mathbf{w} = \begin{pmatrix} \lambda w_1 \\ \lambda w_2 \end{pmatrix}.$$

Considering $\lambda\mathbf{w} = P^\top w$ we obtain the equations

$$\lambda w_1 = \frac{\theta}{\gamma}(\gamma-\theta)w_1,$$
$$\lambda w_2 = \frac{\theta w_1}{1+\alpha\xi+\theta}.$$

Now $\lambda = 0$ implies that $w_1 = 0$ wince $\gamma - \theta \neq 0$ and w_2 is arbitrary. Hence eigen vector of $P^\top$ corresponding the eigen value $\lambda = 0$ is given by

$$\mathbf{w} = \begin{pmatrix} 0 \\ 1 \end{pmatrix} = \begin{pmatrix} w_1 \\ w_2 \end{pmatrix}.$$

From Eq. (26) we have

$$\boldsymbol{f}_\delta(\theta, 0; \delta) = \begin{pmatrix} 0 \\ 0 \end{pmatrix}$$

and hence

$$\mathbf{w}^\top \boldsymbol{f}_\delta(\theta, 0; \delta) = \begin{pmatrix} 0 & 1 \end{pmatrix}\begin{pmatrix} 0 \\ 0 \end{pmatrix} = 0. \tag{28}$$

Now, let us consider

$$\begin{aligned} D\boldsymbol{f}_\delta(x, y; \delta)\mathbf{v} &= \frac{\partial \boldsymbol{f}_\delta(x, y; \delta)}{\partial x}v_1 + \frac{\partial \boldsymbol{f}_\delta(x, y; \delta)}{\partial y}v_2 \\ &= \frac{\partial}{\partial x}\begin{pmatrix} 0 \\ -y \end{pmatrix}v_1 + \frac{\partial}{\partial y}\begin{pmatrix} 0 \\ -y \end{pmatrix}v_2 \\ &= \begin{pmatrix} 0 \\ 0 \end{pmatrix}v_1 + \begin{pmatrix} 0 \\ -1 \end{pmatrix}v_2. \end{aligned} \tag{29}$$

The expansion of the term $D^2\boldsymbol{f}(x, y; \delta)(\mathbf{v}, \mathbf{v})$ is given by

$$\begin{aligned} D^2\boldsymbol{f}(x, y; \delta)(\mathbf{v}, \mathbf{v}) &= \frac{\partial^2 \boldsymbol{f}(x, y; \delta)}{\partial x \partial x}v_1v_1 + \frac{\partial^2 \boldsymbol{f}(x, y; \delta)}{\partial x \partial y}v_1v_2 \\ &\quad + \frac{\partial^2 \boldsymbol{f}(x, y; \delta)}{\partial y \partial x}v_2v_1 + \frac{\partial^2 \boldsymbol{f}(x, y; \delta)}{\partial y \partial y}v_2v_2 \\ &= \begin{pmatrix} \left[-\frac{6x}{\gamma} + 2\left(1+\frac{\theta}{\gamma}\right) + \frac{2(1+\alpha\xi)}{(1+\alpha\xi+x)^3}\right]v_1v_1 \\ \left[\frac{-2[(1+\alpha\xi)\beta y - \beta\xi y]}{(1+\alpha\xi+x)^2}\right]v_1v_1 + 2\left[\frac{\beta[(1+\alpha\xi)-\xi]}{(1+\alpha\xi+x)^2}\right]v_1v_2 \end{pmatrix}. \end{aligned} \tag{30}$$

Evaluating $D\boldsymbol{f}_\delta(x, y; \delta)\mathbf{v}$ at $(x, y) = (\theta, 0)$ using (27) and (29) we obtain

$$\begin{aligned} D\boldsymbol{f}_\delta(x, y; \delta)\mathbf{v} &= \begin{pmatrix} 0 \\ 0 \end{pmatrix}.1 + \begin{pmatrix} 0 \\ -1 \end{pmatrix}\frac{(1+\alpha\xi+\theta)(\gamma-\theta)}{\gamma} \\ &= \begin{pmatrix} 0 \\ -\frac{(1+\alpha\xi+\theta)(\gamma-\theta)}{\gamma} \end{pmatrix} \end{aligned}$$

and hence we have

$$\begin{aligned} \mathbf{w}^\top[D\boldsymbol{f}_\delta(\theta, 0; \delta)\mathbf{v}] &= \begin{pmatrix} 0 & 1 \end{pmatrix}\begin{pmatrix} 0 \\ -\frac{(1+\alpha\xi+\theta)(\gamma-\theta)}{\gamma} \end{pmatrix} \\ &= -\frac{(1+\alpha\xi+\theta)(\gamma-\theta)}{\gamma} \neq 0. \end{aligned} \tag{31}$$

Evaluating $\mathbf{w}^\top D^2\boldsymbol{f}(\theta, 0; \delta)(\mathbf{v}, \mathbf{v})$ using (27) and (30) we obtain

$$\begin{aligned} &\mathbf{w}^\top[D^2\boldsymbol{f}(\theta, 0; \delta)(\mathbf{v}, \mathbf{v})] \\ &= \begin{pmatrix} 0 & 1 \end{pmatrix}\begin{pmatrix} -6\frac{\theta}{\gamma} + 2\left(1+\frac{\theta}{\gamma}\right) + \frac{2(1+\alpha\xi)}{(1+\alpha\xi+\theta)^3} \\ 2\frac{\beta[(1+\alpha\xi)-\xi](\gamma-\theta)}{(1+\alpha\xi+\theta)} \end{pmatrix} \\ &= 2\frac{\beta[(1+\alpha\xi)-\xi](\gamma-\theta)}{(1+\alpha\xi+\theta)} \neq 0. \end{aligned} \tag{32}$$

From Sotomayer theorem [46] together with the Eqs. (28), (31) and (32), the prey-predator system (8)–(9) experiences transcritical Bifurcation at E_θ. In a similar manner, we can also prove that the prey-predator system (8)–(9) experiences transcritical Bifurcation at E_γ

References

1. Kot M (2001) Elements of mathematical ecology. Cambridge University Press, Cambridge
2. Holling CS (1959) The components of predation as revealed by a study of small-mammal predation of the European pine sawfly. Can Entomol 91(5):293–320
3. Holling CS (1965) The functional response of predators to prey density and its role in mimicry and population regulation. Mem Entomol Soc Can 97(suppl. S45):5–60
4. Holling CS (1966) The functional response of invertebarte predators to prey density. Mem Entomol Soc Can 98(suppl. S48):5–86
5. Ruan S, Xiao D (2001) Global analysis in a predator-prey system with nonmonotonic functional response. SIAM J Appl Math 61:1445–1472
6. Aguirre P, Gonzlez-Olivares E, Sez E (2009) Three limit cycles in a Leslie-Gower predatorprey model with additive Allee effect. SIAM J Appl Math 69:1244–1262
7. Gonzalez-Olivares E, Meneses-Alcay Hector, Gonzalez-Yanez Betsabe, Mena-Lorca Jaime, Rojas-Palma Alejandro, Ramos-Jiliberto Rodrigo (2011) Multiple stability and uniqueness of the limit cycle in a Gause-type predatorprey model considering the Allee effect on prey. Nonlinear Anal RWA 12:2931–2942
8. Lidicker WZ Jr (2010) The Allee effect: its history and future importance. Open Ecol J 3:71–82
9. Courchamp F, Clutton-Brock T, Grenfell B (1999) Inverse density dependence and the Allee effect. Trends Ecol Evol 14(10):405–410
10. Berec L, Angulo E, Counchamp F (2006) Multiple Allee effects and population management. Trends Ecol Evol 22(4):185–191
11. Beth FTB, Hassall M (2005) The existence of an Allee effect in populations of Porcellio scaber(Isopoda: Oniscidea). Europ J Soil Biol 4:123–127
12. Frank MH, Langlais M, Sergei VP, Malchow H (2007) A diffusive SI model with Allee effect and application to FIV. Math Biosci 206:61–80
13. Gardner JL (2004) Winter flocking behaviour of speckled warblers and the Allee effect. Biol Conserv 118:195–204
14. Hurford A, Hebblewhite M, Lewis MA (2006) A spatially explicit model for an Allee effect: why wolves recolonize so slowly in Greater Yellowstone. Theor Popul Biol 70:244–254
15. Kuussaari M, Saccheri I, Camara M, Hanski I (1998) Allee effect and population dynamics in the Glanville fritillary butterfly. Oikos 82(2):384–392
16. Penteriani V, Otalora F, Ferrer M (2007) Floater mortality within settlement areas can explain the Allee effect in breeding populations. Ecol Model 213:98–104
17. Correigh MG (2003) Habitat selection reduces extinction of populations subject to Allee effects. Theor Popul Biol 64:1–10
18. Stephens PA, Sutherland WJ (1999) Consequences of the Allee effect for behavior, ecology and conservation. Trends Ecol Evol 14(10):401–405
19. Lin Z-S, Li B-L (2002) The maximum sustainable yield of Allee dynamic system. Ecol Model 154:1–7
20. Hopper KR, Roush RT (1993) Mate finding, dispersal, number released, and the success of biological-control introductions. Ecol Entomol 18:321–331
21. Caz MT, Hastings A (2005) Allee effects in biological invasions. Ecol Lett 8:895–908
22. Chen L-L, Lin Z-S (2008) The effect of habitat destruction on metapopulations with the Allee-like effect: a study case of Yancheng in Jiangsu Province. China Ecol Model 213(3–4):356–364
23. Patric CT, Stefanie LW, Derek MJ, Bjørnstad ON, Andrew ML (2007) Invasion speed is affected by geographical variation in the strength of Allee effects. Ecol Lett 10:36–43
24. Regina CA, Simone AD, da S Costa MI (2006) A numerical model to solve single-species invasion problems with Allee effects. Ecol Model 192:601–617
25. Wang M-H, Kot M (2001) Speeds of invasion in a model with strong or weak Allee effects. Math Biosci 171:83–97
26. Zhou S-R, Liu C-Z, Wang G (2004) The competitive dynamics of metapopulations subject to the Allee-like effect. Theor Popul Biol 65:29–37
27. Zhou S-R, Wang G (2004) Allee-like effects in metapopulation dynamics. Math Biosci 189:103–113
28. David SB, Maurice WS, Berec L (2007) How predator functional responses and Allee effects in prey affect the paradox of enrichment and population collapses. Theor Popul Biol 72:136–147
29. Ferdy J-B, Molofsky J (2002) Allee effect, spatial structure and species coexistance. J Theor Biol 217:413–427
30. Kent A, Doncaster CP, Sluckin T (2003) Consequences for predators of rescue and Allee effects on prey. Ecol Model 162:233–245
31. van Kooten T, de Roos AM, Persson L (2005) Bistability and an Allee effect as emergent consequeences of stage-specific predation. J Theor Biol 237:67–74
32. Zhou S-R, Liu Y-F, Wang G (2005) The Stability of predator-prey systems subject to the Allee effects. Theor Popul Biol 67:23–31
33. David SB, Berec L (2002) Single-species models of the Allee effect: extinction boundaries, sex ratios and mate encounters. J Theor Biol 218:375–394
34. Aguirre P, Gonzalez-Olivares E, Soledad Torres E (2013) Stochastic predatorprey model with Allee effect on prey. Nonlinear Anal RWA 14:768–779
35. Cai Y, Wang W, Wang J (2012) Dynamics of a diffusive predator-prey model with additive Allee effect. Int J Biomath 5(2):1250023
36. Hadjiavgousti D, Ichtiaroglou S (2008) Allee effect in a preypredator system. Chaos Solitons Fractals 36:334–342
37. Gonzalez-Olivares E, Gonzalez-Yanez B, Lorca JM, Rojas-Palma Alejandro, Flores Jose D (2011) Consequences of double Allee effect on the number of limit cycles in a predatorprey model. Comput Math Appl 62:3449–3463
38. Gonzlez-Olivares E, Mena-Lorca Jaime, Rojas-Palma Alejandro, Flores Jos D (2011) Dynamical complexities in the LeslieGower predatorprey model as consequences of the Allee effect on prey. Appl Math Model 35:366–381
39. Sun Gui-Quan, Jin Zhen, Li Li, Liu Quan-Xing (2009) The role of noise in a 495 predatorprey model with Allee effect. J Biol Phys 35:185–196
40. Sen M, Banerjee M, Morozov A (2012) Bifurcation analysis of a ratio-dependent preypredator model with the Allee effect. Ecol Complex 11:12–27
41. Courchamp F, Berec L, Gascoigne J (2008) Allee effects in ecology and conservation. Oxford University Press, Oxford
42. Srinivasu PDN, Prasad BSRV, Venkatesulu M (2007) Biological control through provision of additional food to predators: a theoretical study. Theor Popul Biol 72:111–120
43. Srinivasu PDN, Prasad BSRV (2010) Time optimal control of an additional food provided predator-prey system with applications to pest management and biological conservation. J Math Biol 60:591–613
44. Srinivasu PDN, Prasad BSRV (2010) Erratum to: time optimal control of an additional food provided predator-prey system with applications to pest management and biological conservation. J Math Biol 61:591–613
45. Srinivasu PDN, Prasad BSRV (2011) Role of quantity of additional food to predators as a control in predator-prey systems with relevance to pest management and biological conservation. Bull Math Biol 73:2249–2276
46. Perko L (2001) Differential equations and dynamical systems. Springer, New York